Anthropogenic climate change doubled the frequency of compound drought and heatwaves in low-income regions

Check for updates

Boen Zhang[1,2], Shuo Wang [2,3] ✉ & Louise Slater [1]

Compound drought-heatwaves have garnered widespread attention due to their catastrophic consequences. However, little research has investigated inequalities in exposure to compound drought-heatwaves under climate change. Here, we reveal a significant disparity between low-income and high-income regions in terms of global compound drought-heatwave occurrence using observations and climate models. We find that low-income regions experienced a 377% [351–403%] increase in the frequency of compound drought-heatwaves from 1981 to 2020, which is twice as fast as the increase observed in high-income regions (184% [153–204%]). This inequality is largely attributed to a similar disparity in drought occurrence rather than heatwave occurrence. Climate change attribution suggests that anthropogenic warming has doubled the frequency of compound drought-heatwaves over 31% [14–50%] of low-income regions, compared to only 4.7% [0.9–8.3%] of high-income regions. The frequency of compound drought-heatwaves would not have increased in low-income regions without anthropogenic climate change but would still have risen in high-income regions.

Climate shocks cause an average of over $300 billion in direct asset losses and approximately 30,000 deaths every year[1,2]. Droughts and heatwaves are among the climate shocks that lead to the largest human losses, accounting for more than 50% of climate-related deaths[3,4]. There are rising concerns regarding the frequent occurrence of compound events, which typically result in disproportionate impacts to agriculture, ecosystems, health, and energy[5]. For example, compound drought-heatwave events (CDHWs) caused a total of approximately 40,000 deaths and a 25% loss of annual crop yield[6] in Europe and western Russia in the summers of 2003 and 2010. CDHWs often cause extensive damages and deaths in lower-income countries, where infrastructure systems tend to be less developed and the agricultural sector tends to be the primary source of employment[7–9]. Recent CDHWs in countries as diverse as Kenya[10], Tunisia[11], Vietnam[12], the United States[13], and Russia[14] illustrate that the threat is a global reality. Rare and major CDHWs can cause food crises and revert years of progress in poverty reduction and development[15].

CDHWs have received much attention around the world, especially in developed regions where record-breaking CDHWs are well documented[16,17]. The frequency of CDHWs has increased markedly across the United States and Eastern China over recent decades[18]. The Sixth Assessment Report (AR6) of the Intergovernmental Panel on Climate

Change (IPCC) also finds high confidence of increased CDHW frequency in the last century as a result of anthropogenic climate change[19]. Yet, CDHW dynamics in low-income regions remain unclear although these regions have experienced major CDHWs. Compared to developed countries, developing countries are particularly susceptible to the effects of CDHWs due to high reliance on agriculture, limited water resources, weak infrastructure, and vulnerable populations. For example, an unprecedented drought compounded with repeated heatwaves hit the Horn of Africa from October 2020 to October 2023, leading to a total of approximately 43,000 deaths in Somalia last year alone, with half of the fatalities among children younger than 5 years of age[20]. Although previous studies have revealed the global increases in CDHW occurrence[3,21], our understanding of such increases across the socioeconomic spectrum is incomplete.

In addition to the historical changes in the CDHW occurrence, a few studies have attempted to assess the influence of anthropogenic climate change on CDHW in light of its severe impacts on socioeconomic development[16,22,23]. For example, one study revealed the positive effect of anthropogenic global warming on CDHW in the top 10 most vulnerable climate regions[24]. However, it remains unclear whether such impacts are felt equally across the planet. Inequality in the impacts of anthropogenic climate change on CDHW would raise critical questions of international justice

[1]School of Geography and the Environment, University of Oxford, Oxford, UK. [2]Department of Land Surveying and Geo-Informatics, The Hong Kong Polytechnic University, Hong Kong, China. [3]Research Institute for Land and Space, The Hong Kong Polytechnic University, Hong Kong, China. ✉ e-mail: shuo.s.wang@polyu.edu.hk

since historical increases in greenhouse gas emissions largely result from wealthy countries[25]. It is thus crucial to compare anthropogenic impacts on CDHW across the socioeconomic spectrums.

Here we present an in-depth assessment of historical changes in global CDHWs across the socioeconomic spectrum to address the aforementioned limitations. Using multiple observational products, we demonstrate that although the CDHW occurrences have risen significantly in regions with varying income levels from 1981 to 2020, they rose twice as fast in low-income regions as in high-income ones. This inequality is most likely due to the unequal growth rates of drought occurrences between low-income and high-income regions. We then utilize the Historical and Natural climate simulations from the Coupled Model Intercomparison Project, Phase 6 (CMIP6) to assess inequalities in the impacts of anthropogenic climate change on CDHWs across the socioeconomic spectrum. Employing quantitative detection and attribution techniques, we find that human-induced climate change is the driving factor behind the heightened frequency of CDHWs in low-income regions, whereas high-income regions would have observed an increase in CDHW frequency even without anthropogenic influence. By offering global insights into CDHWs and poverty, this study highlights the necessity of providing further support to low-income countries to address the increasing threat of compound events and to reduce inequalities in climate change-attributed increases in CDHWs.

Results

Unequal increases in CDHW events

We used the weekly self-calibrated Palmer Drought Severity Index (scPDSI) and daily maximum temperatures derived from multiple observation products to identify summer CDHWs during the period 1981 to 2020 (see "Methods"). We find that the CDHWs have been increasing significantly ($P < 0.05$) over approximately 57% of global land areas, and these regions are home to approximately 3.94 billion people, mainly located in Africa (40%), East Asia (33%), Latin America (8%), and the Middle East (4%) (see Fig. 1a generated from the ERA5 reanalysis). Our results also suggest a prominent spatial difference in the growth rate of CDHW occurrence and inequality globally (Fig. 1b). Such difference is statistically significant at the 5% significance level based on 500 bootstrap resampling and a two-tailed t-test (Fig. 1c). Low-income regions are experiencing significantly ($P < 0.05$) more rapid increases in CDHWs than high-income regions (following the WorldBank's 2020 income classification). CDHWs in low-income regions have increased by 317% [257–377%] between the earlier and later periods (1981–2000 and 2001–2020) in the last 40 years, but the increase is only 127% [70–184%] in high-income regions, especially in the United States (USA) and Europe where the increases in the frequency of CDHWs are only 55% [14–87%] and 73% [39–113%], respectively. In addition, accounting for the uncertainty of precipitation and temperature datasets, we find that there is a consistent difference between the high-income and low-income regions in the growth rates of CDHW occurrence based on multiple datasets (see Fig. 1b and Supplementary Figs. 1–3). Although the growth rates of CDHW occurrence in tropical Africa, home to some low-income and lower-middle-income countries, may vary with the datasets used, consistent increases are observed across all datasets.

In addition, there is a strong dependence between historical changes in CDHWs and the fraction of population living in extreme poverty (i.e., on less than $1.90 per day), with a Pearson correlation coefficient of 0.653 ($P = 0.002$; see Fig. 1d). This is estimated through aggregating locations by ventiles (i.e., 20-quantiles) of the poverty rate from the latest edition of the World Bank's Global Subnational Atlas of Poverty (GSAP) and by graphing the changing rate of CDHW occurrences. CDHWs show an approximately twofold increase (222% on average) in locations where the share of population living in extreme poverty is lower than 10% between the early and later halves of 1981–2020. In comparison, locations where the share of population living in extreme poverty is higher than 90% are experiencing a nearly fivefold increase (482%), on average, in the frequency of CDHWs. Such a dependence becomes even stronger, with Pearson correlation

coefficients of 0.787 and 0.790 (see Supplementary Fig. 4), if we consider the less stringent poverty definitions of $3.20 and $5.50 per day, respectively. In addition to the frequency of CDHWs, similar inequalities also exist for the historical changes in the severity of CDHWs (see Supplementary Fig. 5).

### Drought dominates the unequal increases of CDHW events

To explain the unequal increases of CDHW events across the socio-economic spectrum, we analyzed historical changes in the annual frequency of droughts and heatwaves over the high-income (HIC) and low-income (LIC) regions. All the datasets show statistically significant ($P < 0.01$) increases in the annual frequency of both droughts and heatwaves (see Fig. 2a–b). We show there is no obvious difference between the HIC and LIC regions in terms of the growth rate for heatwaves, with slope values of 1.3% and 2.2% per year, respectively (Fig. 2a). In comparison, a large difference is observed for droughts, with slope values of 1.9% and 4.3% for the HIC and LIC regions, respectively (Fig. 2b).

In addition, bootstrapping and t-test were also used to assess the statistical significance of the difference between the HIC and LIC regions in terms of historical changes in the drought and heatwave occurrences. We find that there is no consistently significant difference in terms of heatwaves based on three datasets. Specifically, although the ERA5 and MERRA-2 temperature datasets show a significant ($P < 0.01$) difference in terms of heatwaves, the CPC temperature dataset shows an insignificant ($P = 0.56$) difference (Fig. 2c). In comparison, all the combinations of precipitation and temperature datasets show a significant ($P < 0.01$) difference between the HIC and LIC regions in terms of droughts (Fig. 2d). For example, the average growth rates in drought occurrence based on the MERRA-2 temperature and ERA5 precipitation are 1.6% and 3.8% over the HIC and LIC regions, respectively. Therefore, one potential explanation for the differing trends in CDHWs between LIC and HIC regions is the similar inequality in drought occurrence rather than heatwave occurrence.

Unequal influence of anthropogenic climate change on CDHWs

We also analyzed the impacts of anthropogenic climate change on the frequency of CDHWs. We quantified the impacts by estimating the likelihood of CDHW occurrences that can be attributed to anthropogenic climate change. The probability ratio concept was used to quantify the likelihood of CDHWs occurring in historical conditions relative to natural-only conditions[26]. Figure 3a displays probability distributions of the probability ratio derived using land pixels for each income group and shows a general increase in the frequency of CDHWs under historical conditions relative to historical natural-only conditions (i.e., probability ratios generally greater than 1). We find a contrasting inequality in the effects of anthropogenic climate change on the frequency of CDHWs between poorer and wealthier countries. Specifically, 31% [14–51%] of land pixels in low-income regions show more than double increases in the frequency of CDHWs due to anthropogenic forcing, versus only 4.7% [0.9–8.3%] of land in high-income regions (Fig. 3a). We find a statistically significant ($P < 0.05$) association between the magnitude of anthropogenic impacts on CDHWs and the share of population living in extreme poverty (living under $1.90 per day), with a Pearson correlation coefficient of 0.764 (Fig. 3b). Such a dependence remains if one considers a higher poverty threshold of $3.20 (or $5.50) (see Supplementary Fig. 6).

The upward trends in the frequency of CDHWs over low-income and high-income countries are well reproduced by the state-of-the-art CMIP6/ALL multi-model ensemble simulations (Fig. 4a and b). The ALL simulations consider both anthropogenic climate forcings, such as the emission of greenhouse gases and aerosols, and natural climate forcings like solar and volcanic activities. The upward trends over high-income countries are also captured by the CMIP6/NAT ensemble simulations, which solely account for natural climate forcings ($P < 0.01$). However, the trends over the low-income countries are not replicated by the CMIP6/NAT ensemble simulations ($P = 0.279$). This indicates that the increase in the frequency of CDHWs in low-income countries during the past 40 years is driven predominantly by anthropogenic climate change.
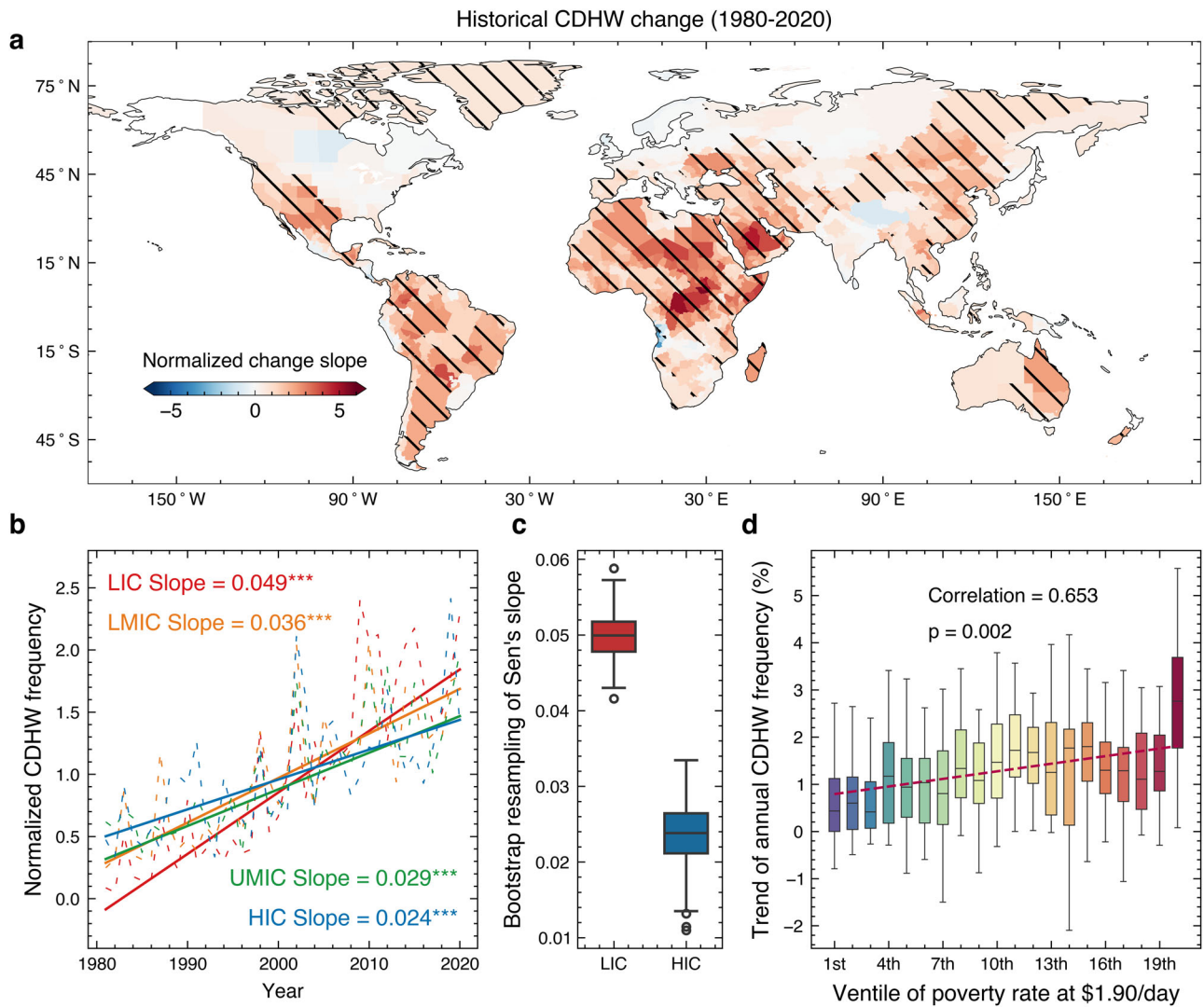
Fig. 1 | Historical increases in CDHW occurrences across different income groups. a Historical trends in the normalized frequency of CDHWs generated from the ERA5 reanalysis dataset at the subnational level during the period of 1981–2020. The frequency was normalized by calculating annual values as a fraction of the 1981–2020 local mean before estimating the historical trend. The slope (unit: year^{-1}) is the linear trend based on Sen's slope estimator. Hatching indicates regions where the trend is significant at the 0.05 level based on a Mann–Kendall (MK) test. **b** Time series of CDHWs spatially aggregated for four different income groups (see map in Supplementary Fig. 12; HIC = high-income countries. UMIC = upper middle-income countries. LMIC = lower-middle-income countries. LIC = low-income countries). Dashed lines represent annual normalized occurrences of CDHWs, and solid lines represent the MK trend based on the MK test. The slope and *p*-value are the same as those in (**a**). **c** presents the 500 bootstrap samples of Sen's slope estimates for the annual frequency of CDHWs for HIC and LIC regions. **d** Global inter-relationships between the share of population that is poor ($1.90 per day) and changes in the frequency of CDHWs. Box extents in (**c**, **d**) are at the 25th and 75th percentiles while the whiskers extend to the 2.5% and 97.5% percentiles. The red dashed line represents the fitted linear regression between poverty rates (x-axis) and median values of CDHW change (y-axis).

We further used an optimal fingerprinting approach (see Methods) to estimate contributions from anthropogenic (ANT) and natural forcings (NAT) to the observed changes in the frequency of CDHWs. The statistically significant non-zero scaling factors for ANT (ALL-NAT; anthropogenic forcings) indicate that the ANT signal is detectable across all four income groups (Fig. 4c). However, the NAT signal shows different results for poorer (LIC and LMIC) and wealthier (UMIC and HIC) countries. The inclusion of zero within the uncertainty range of scaling factors suggests a failure to detect NAT forcings in poorer countries, whereas the exclusion of zero in wealthier countries implies the detectability of NAT forcings. In other words, although anthropogenic climate change has contributed to the past increases in CDHW occurrences, the magnitude of such contributions is larger in regions with lower-income levels. Specifically, the ANT-forced increases in the frequency of CDHWs are 19% [2–33%], 18% [6–26%], 17% [9–23%], and 12% [5–18%] per decade for low-income, lower-middle-

income, upper-middle-income, and high-income countries, respectively, during the period of 1981–2020. We therefore conclude that anthropogenic climate change has made a larger contribution to the increases in the frequency of CDHWs in poorer countries than in wealthier countries.

Discussion

The IPCC Sixth Assessment Report (AR6) indicates that CDHW events have increased in nearly all land regions under global warming, but it remains unclear whether inequality exists in the historical changes of CDHW events across socioeconomic levels. Our findings indicate that low-income regions and countries are experiencing a faster increase in the frequency and severity of CDHWs than middle- and high-income regions. CDHWs are also growing twice as fast as the independent heatwave and drought events (Supplementary Fig. 7). Poor regions are often less well-equipped to cope with the increase in CDHWs due to their more limited
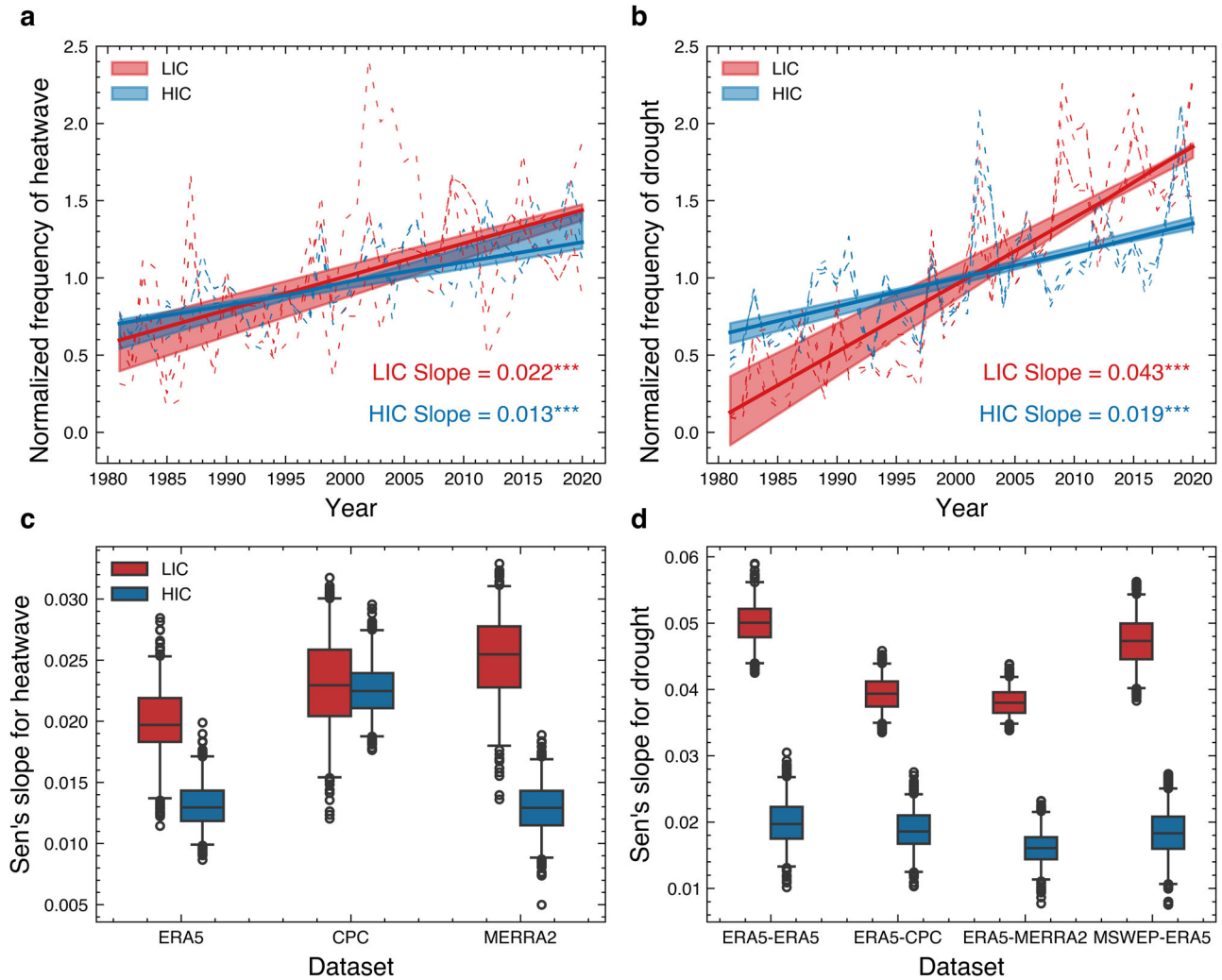
Fig. 2 | Historical changes in the annual frequency of heatwaves and droughts for the high-income (HIC) and low-income (LIC) regions. Dashed lines in (a, b) represent annual normalized occurrences of droughts and heatwaves, respectively. The shaded regions represent the lower and upper ranges of Sen's estimates, taking into account the uncertainty of meteorological datasets (i.e., ERA5 and MSWEP datasets for precipitation; ERA5, CPC, and MERRA-2 datasets for temperature). The solid lines represent the median values of Sen's estimates generated from different meteorological datasets. The slope (unit: year^{-1}) is Sen's slope estimate. *** indicates the trend is significant at the 0.01 level based on a Mann–Kendall (MK) test. **c, d** Present the boxplots of the 500 bootstrap samples of Sen's slope estimates for the annual frequency of heatwaves and droughts, respectively, for the HIC and LIC regions. The box extents and whiskers in (c, d) are the same as those in Fig. 1.

Fig. 3 | Anthropogenic climate change impacts on the frequency of CDHWs across different income groups. Here, the probability ratio (PR) is used to quantify the impacts of anthropogenetic forcing on the frequency of CDHWs during the period of 1981–2020 (see Methods). **a** Each probability density function represents the PR distribution for an income group and the percentage indicates the fraction of regions in the HIC and LIC groups that have experienced more than double in the anthropogenic impacts on CDHWs. **b** Global interrelationship between the share of population that is poor ($1.90 per day) and anthropogenic climate change impacts on the frequency of CDHWs (i.e., the PR). The box extents and whiskers in **b** are the same as those in Fig. 1. The red dashed line represents the fitted linear regression between poverty rates (x-axis) and the PR (y-axis). The Pearson correlation coefficient and its *p*-value are shown.
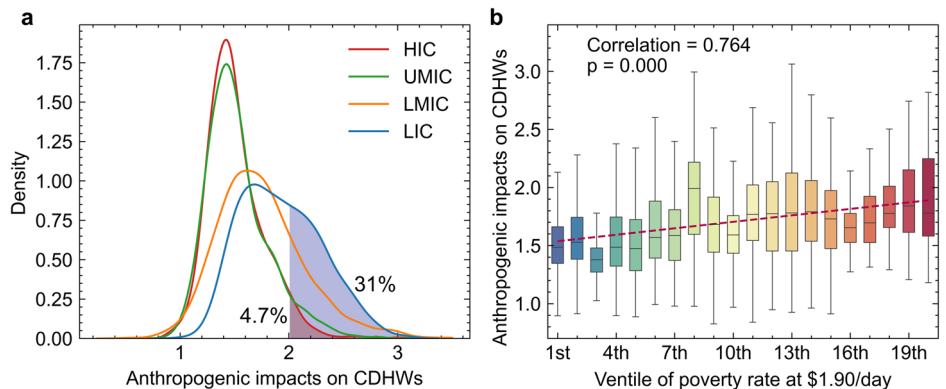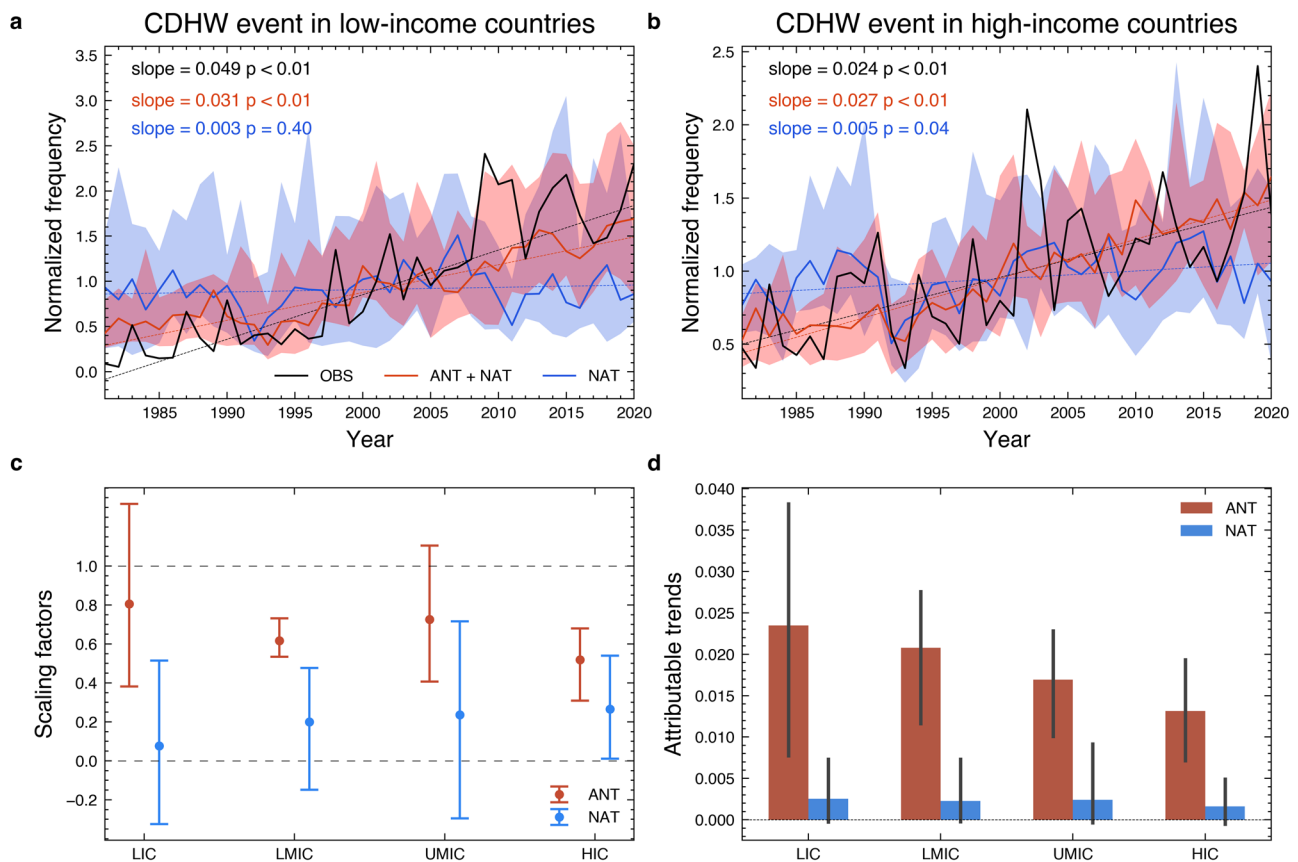
Fig. 4 | Attribution of changes in CDHW across different income groups. Observed and simulated frequencies of CDHWs for **a** low-income and **b** high-income countries from 1981 to 2020. The solid black line in (**a**, **b**) indicates the annual frequency of CDHWs based on the ERA5 reanalysis dataset (OBS), and solid orange and green lines represent the ensemble mean results based on CMIP6 climate model simulations with ALL (ANT + NAT) and NAT forcings, respectively (Supplementary Table 1). The dashed lines represent the linear trend, and the shadings show the 5 to 95% ranges based on the ensemble simulations of ALL and NAT, respectively. **c** The best estimates of the scaling factors for each income group and (**d**) attributable increasing trends (unit: %/year) generated from a two-signal [ANT (ALL-NAT) and NAT] analysis of changes in the frequency of CDHWs spanning from 1981 to 2020. The error bars in (**c**, **d**) illustrate the uncertainty range of 5 to 95% for the respective estimates. The frequency is calculated for each grid cell and then weighted by the area of grid cells for different income groups with consideration of the weights assigned to grid areas. The frequency is calculated for each year as the area-weighted average of grid cells in different income groups.

resources and forecasting capacities. Poverty exposure to an increased frequency of CDHWs can exacerbate worker productivity losses and reduce crop yields, pushing vulnerable households further into poverty and hampering economic development in poor regions. We also identified a contrasting difference in historical trends in the frequency of CDHWs between Global South and North regions. Regions of the Global North have experienced only one-third of the increase in the frequency of CDHWs experienced by regions of the Global South (Supplementary Fig. 8). These detected spatial differences could put at risk the achievement of the United Nations' Sustainable Development Goals which are to reduce poverty (Goal 1) and inequality within and between nations (Goal 10), as well as to take urgent actions to combat climate change impacts (Goal 13).

The unequal historical increases in CDHW events across the socioeconomic spectrum can be largely attributed to the similar disparity in drought occurrence rather than heatwave occurrence. Accounting for the uncertainty of air temperature datasets, we find no significance in the growth rates of heatwave occurrences between the high-income and low-income regions. This is inconsistent with previous studies, which reveal that populations in lower-income regions currently face a higher exposure to heatwaves than those in higher-income regions[27]. In comparison, all the datasets show a statistically significant difference between the high-income and low-income regions in terms of historical changes in drought occurrence. This suggests that efforts to eliminate exposure inequality to compound dry-hot events would benefit more from targeting the exposure inequality of droughts than that of heatwaves.

Anthropogenic climate change has contributed to increases in the frequency and severity of CDHWs globally (Supplementary Figs. 9 and 10). However, our findings reveal that the effect of climate change is felt mostly by low- and lower-middle-income regions since high- and middle-high-income regions would have experienced an increase in the frequency of CDHWs even without anthropogenic influences. By contrast, there is a significant anthropogenic influence on the increase in the frequency of CDHWs for low-income regions. Thus, our findings provide evidence of social inequalities in the impacts of climate change on CDHW occurrences. Although developed and wealthy countries contribute substantially (~60–80%[25,28]) to the global temperature rise, such anthropogenic emissions do not appear to affect the occurrence of CDHWs in these countries. Instead, they have a greater impact on regions with higher poverty rates, especially African countries[29].

Previous studies have mostly focused on individual extreme climate events such as heatwaves[27] and floods[30] to analyze whether climate change might have inequitable social impacts. Mounting evidence has shown that concurrent occurrences of multiple extreme climate events are becoming more frequent in a changing climate, with the potential to cause severe socioeconomic impacts[31]. Our findings uncover the climate injustice in the occurrence of CDHWs between poorer and wealthier countries. We argue that an equally important line of inquiry should focus on how climate-induced increases in compound events are having unequal social impacts[32].

While the specific results of this study might vary depending on the time period chosen, the overall conclusion of exposure inequality in the

CDHW event would remain unchanged. By using only 30 years of data (1991–2020), we have still revealed the unequal increases in CDHW events (see Supplementary Fig. 11). In addition, previous studies also directly and indirectly reinforce the conclusion. For example, Hao et al. assessed changes in the frequency of CDHEs between the two periods 1951–1984 and 1985–20181, and their global result showed that poor regions experienced greater increases than wealthy ones although they did not provide a detailed comparison analysis[6]. Our findings reveal that drought dominates the unequal increases of CDHW events, and Winsemius et al.'s study showed poor people are disproportionally exposed to droughts in 52 countries during the period of 1960–1999[33].

Methods

Reanalysis and climate simulations

We use daily precipitation (P), daily maximum and minimum 2-meter air temperature (Tmax and Tmin) datasets obtained from the European Centre for Medium-Range Weather Forecasts Reanalysis 5 (ERA5), available at 0.25° spatial resolution for the period of 1981–2020. The ERA5 dataset supersedes other reanalysis products due to its high spatial and temporal resolutions[34]. Previous work has shown that it provides spatially robust estimates of CDHW characteristics[4,35]. In addition, the daily Multi-Source Weighted-Ensemble Precipitation (MSWEP) dataset is used to consider the uncertainty of precipitation datasets[36]. The Modern-Era Retrospective Analysis for Research and Applications, Version 2 (MERRA-2)[37] and Climate Prediction Center (CPC)[38] datasets are used to consider the uncertainty of temperature datasets. Available water-holding capacity of the soil is obtained from a soil texture-based global water-holding-capacity map[39] and regridded into 0.25° spatial resolution based on nearest neighbor interpolation.

Daily precipitation, Tmax, and Tmin datasets from an ensemble of 10 climate model outputs of the Coupled Model Intercomparison Project Phase 6 (CMIP6) experiment are used in the historical simulations (Supplementary Table 1) spanning from 1981 to 2020 under two scenarios, including those based on all forcings (ALL: both natural and anthropogenic forcings) and natural forcings (NAT). The 10 climate model outputs are selected since most of them have relatively fine spatial resolution. Given that CMIP6 ALL data ends in 2014, we merge the years 2015 to 2020 from the intermediate emission scenario (SSP245) with the years 1981 to 2014 from the ALL simulation since previous studies show that SSP245 and SSP585 have a similar temporal pattern in droughts and temperature during the period of 2015–2020[40,41]. The examination of ALL and NAT simulations provides insight into the influence of anthropogenic factors. To ensure consistency, all the simulation datasets are regridded into a spatial resolution of 1° × 1°. For our analysis, we calculate the multi-model average of historical simulations, which helps mitigate internal variability and emphasizes the predominantly forced signals in the aggregated model response.

Administrative boundaries and poverty estimates

This study utilizes the latest edition of the Global Subnational Atlas of Poverty (GSAP) and the classification of countries by income group from the World Bank to characterize global poverty. The GSAP, updated in 2020, provides statistically representative poverty estimates for various subnational units, which are typically provinces or states but may include custom groupings determined by household survey sampling strategies. To ensure accuracy, small subnational units in the GSAP that are too small for a 0.25° × 0.25° grid are aggregated into larger units that cover at least five grids (approximately 300 km²) within each country. Consequently, isolated small units like the Cayman Islands are excluded from the analysis. In total, 843 subnational units in 169 countries are covered in this study. In addition, the World Bank's country classification leads to four income groups, including low, lower-middle, upper-middle, and high-income countries. The four income groups are assigned based on the gross national income per capita and the classifications in 2020 are used in this study (see Supplementary Fig. 12).

The GSAP offers poverty and income estimates for each subnational unit, which are derived from the latest available Living Standards Measurement Survey for the respective country[42]. We assume hazard exposure is uniform across income groups within a region since we apply poverty rates at the subnational administrative level. Such an approach may overestimate the exposure of low-income households to increases in CDHW events. For example, a significant increase in CDHW occurrence is observed in a subnational region of Niger, where nearly 0.68 million people reside and 30% of population lives in poverty ($1.90 per day). Our estimate would suggest that 0.2 million poor people are exposed to increases in CDHW occurrence in this region. However, such estimates are likely to be overestimated due to the uneven distributions of wealth and CDHW events within the region. Therefore, the estimates in this study regarding the exposure of the population in poverty to CDHW events should be interpreted as upper-bound estimates. The study follows the standard World Bank definition of poverty to calculate poverty rates in each subnational administrative unit, using daily expenditure thresholds of $1.90, $3.20, and $5.50. For clarity, all monetary values in this study are denoted in United States dollars (USD).

Identification of CDHW events

This study focuses on summer CDHW events by integrating heatwave and drought information. Specifically, a drought event is identified based on the weekly self-calibrated Palmer Drought Severity Index (scPDSI)[43], which incorporates weekly potential evapotranspiration (PET), weekly total precipitation, and available water holding capacity as inputs. The PET is estimated based on weekly mean temperature (average of Tmax and Tmin) through Thornthwaite's method[44]. The scPDSI is derived using the characteristics of the local climate calibrated based upon the entire period from 1981 to 2020. A heatwave event is identified based on the abnormally high-temperature anomalies observed for at least three consecutive days. Here, the abnormally high-temperature anomalies are defined as the positive difference between Tmax and its 90th percentile. To account for potential epidemiological significance[45], two successive heatwave events are considered independent if there is a minimum of four days between them; otherwise, they are grouped into a single event.

To estimate the CDHW events, we identify time periods of three or more consecutive days when a heatwave event coincides with extreme drought weeks[46]. An extreme drought week is determined when the scPDSI magnitude falls below the 10th percentile of the weekly values for the entire study period[3]. A heatwave event is identified as a spell of at least three consecutive days when Tmax exceeds the 90th percentile threshold[4,45]. The 90th percentile of Tmax is calculated separately for each location in the extended summer seasons (May–October in the Northern Hemisphere, and November–April in the Southern Hemisphere). By using the 95th percentile of Tmax, we show the choice of temperature threshold does not affect the conclusion regarding the unequal historical increases in CDHW events across the socioeconomic spectrum (Supplementary Fig. 13).

The CDHW events are characterized in terms of their frequency and severity. The frequency of CDHW events represents the average number of annual events during the study period, while the severity is calculated based on the cumulative sum of daily severity values obtained over the consecutive days of CDHW events. Daily severity is determined by multiplying the daily standardized values of maximum temperatures with the scPDSI value observed during the coincident extreme drought week[3].

Population data

We utilize the WorldPop Global High Resolution Population dataset (WPGP) generated by the University of Southampton, the World Bank, and other partners. This dataset offers comprehensive global coverage and is accessible on an annual basis spanning from 2000 to 2020. While WorldPop comprises various datasets encompassing poverty, demographics, and urban change mapping, our focus lies on the high-resolution population density map (WorldPop-PPP-2020). This particular dataset presents the population count per individual 3-arcsecond cell in raster format. The data utilized for this purpose is primarily derived from administrative or census-based population records that have been disaggregated into grid cells based

on the spatial arrangement and density of built-up areas derived from satellite imagery.

Statistical significance

The Mann–Kendall (MK) trend test is used to determine if the frequency and severity of CDHWs have a statistically significant trend at a significance level of 0.05 and the Sen's slope is used to estimate the rate of change. This approach is a nonparametric test, so the samples are not required to follow a specific distribution. The null hypothesis in the MK test is that there is no monotonic trend in the series and the alternative hypothesis is that the data has a monotonic trend (positive or negative). 500 bootstrap resampling of Sen's slope and a two-tailed t-test are used to determine if a statistically significant difference exists between LIC and HIC regions in terms of historical trends in the frequency and severity of CDHWs.

Formal detection and attribution

We utilize an optimal fingerprinting method to effectively identify and attribute observed changes in the frequency of CDHWs[47]. The observed changes (y) are expressed as a combination of scaled fingerprints (X) of various external drivers, along with internal climate variability (ε)

$$y = \beta X + \varepsilon \qquad (1)$$

To construct the fingerprints, we use the multi-model ensemble mean of forced simulations while relying on outputs from pre-industrial control runs to estimate internal climate variability. These fingerprints, both in terms of frequency and severity, are then pre-processed into nonoverlapping 2-year-mean time series comprising of 20 data samples spanning the period from 1981 to 2020. The anthropogenically forced signal (ANT) is determined as the disparity between the multi-model ensemble mean responses to ALL and NAT (natural) forcings. The regression coefficients (scaling factors) β are used to scale the fingerprints and optimize their fit to the observed changes.

In order to fit and test the regression models, two independent estimates are required for the inversed covariance structure of internal climate variability. Specifically, the pre-industrial control simulations are divided into 40 nonoverlapping segments and then separated into two sets. These sets are used to accomplish data pre-whitening and estimate the 5–95% uncertainty range of scaling factors, respectively. To determine the covariance matrix of internal climate variability, a regularized estimate is conducted to generate a full-rank covariance matrix, thereby mitigating the underestimation of the lowest eigenvalues that may occur in the original covariance matrix.

If the scaling factor for a specific external forcing is significantly larger than zero, the response to that forcing is considered detectable in the observed changes. A scaling factor of unity indicates that the multi-model ensemble mean of forced responses aligns with the observations[48]. When the scaling factor is smaller (larger) than one, it signifies that the simulations overestimate (underestimate) the magnitude of responses to this forcing compared to the observations. The attributable portion in observed trends of frequency and severity is calculated as the product of simulated linear trends for these characteristics and their respective scaling factors. The 5–95% uncertainty range of attributable changes is then determined by multiplying the ensemble mean forced changes with the uncertainty range of corresponding scaling factors.

Data availability

All datasets used in this study are publicly available. The ERA5 reanalysis dataset is available at https://doi.org/10.24381/cds.adbb2d47. The MSWEP dataset is available at https://www.gloh2o.org/mswep/. The CMIP6 model outputs are available at https://esgf-node.llnl.gov/projects/cmip6/. The population density map (WorldPop-2000) is publicly available at https://hub.worldpop.org/project/categories?id=3. The latest edition of the World Bank's GSAP is available at https://maps.worldbank.org.

Code availability

The code used for this study is available at https://github.com/zhangboen/cdhw_poverty.git.

References

1. Baez, J. E., Caruso, G. & Niu, C. Extreme weather and poverty risk: evidence from multiple shocks in Mozambique. *Econ. Disasters Clim. Chang.* **4**, 103–127 (2020).
2. Marotzke, J., Semmann, D. & Milinski, M. The economic interaction between climate change mitigation, climate migration and poverty. *Nat. Clim. Chang.* **10**, 518–525 (2020).
3. Mukherjee, S. & Mishra, A. K. Increase in compound drought and heatwaves in a warming world. *Geophys. Res. Lett.* **48**, e2020GL090617 (2021).
4. Yin, J. et al. Future socio-ecosystem productivity threatened by compound drought–heatwave events. *Nat. Sustain.* **6,** 259–272 (2023).
5. Zhou, S., Zhang, Y., Williams, A. P. & Gentine, P. Projected increases in intensity, frequency, and terrestrial carbon costs of compound drought and aridity events. *Sci. Adv.* **5**, eaau5740 (2019).
6. Hao, Z. et al. Compound droughts and hot extremes: Characteristics, drivers, changes, and impacts. *Earth-Science Rev.* **235**, 104241 (2022).
7. Gazzotti, P. et al. Persistent inequality in economically optimal climate policies. *Nat. Commun.* **12**, 3421 (2021).
8. Callahan, C. W. & Mankin, J. S. Globally unequal effect of extreme heat on economic growth. *Sci. Adv.* **8**, eadd3726 (2022).
9. Sager, L. Highly unequal carbon footprints. *Nat. Sustain.* **5**, 912–913 (2022).
10. Weber, T. et al. Analysis of compound climate extremes and exposed population in Africa under two different emission scenarios. *Earth's Futur.* **8**, e2019EF001473 (2020).
11. Vogel, J., Paton, E., Aich, V. & Bronstert, A. Increasing compound warm spells and droughts in the Mediterranean Basin. *Weather Clim. Extrem.* **32**, 100312 (2021).
12. Hao, Z., Hao, F., Singh, V. P. & Zhang, X. Changes in the severity of compound drought and hot extremes over global land areas. *Environ. Res. Lett.* **13**, 124022 (2018).
13. Alizadeh, M. R. et al. A century of observations reveals increasing likelihood of continental-scale compound dry-hot extremes. *Sci. Adv.* **6**, eaaz4571 (2020).
14. Schumacher, D. L. et al. Amplification of mega-heatwaves through heat torrents fuelled by upwind drought. *Nat. Geosci.* **12**, 712–717 (2019).
15. Hubacek, K., Baiocchi, G., Feng, K. & Patwardhan, A. Poverty eradication in a carbon constrained world. *Nat. Commun.* **8**, 912 (2017).
16. Ionita, M., Caldarescu, D. E. & Nagavciuc, V. Compound hot and dry events in Europe: variability and large-scale drivers. *Front. Clim.* **3**, 688991 (2021).
17. Ghanbari, M., Arabi, M., Georgescu, M. & Broadbent, A. M. The role of climate change and urban development on compound dry-hot extremes across US cities. *Nat. Commun.* **14**, 3509 (2023).
18. Mazdiyasni, O. & AghaKouchak, A. Substantial increase in concurrent droughts and heatwaves in the United States. *Proc. Natl. Acad. Sci. USA.* **112**, 11484–11489 (2015).
19. Seneviratne, S. I. et al. Weather and climate extreme events in a changing climate. in *Climate Change 2021: The Physical Science Basis. Contribution of Working Group I to the Sixth Assessment Report of the Intergovernmental Panel on Climate Change* (Cambridge University Press, 2021).
20. Harris, E. Drought caused 43 000 deaths in Somalia in 2022, half among children. *Jama* **329**, 1249 (2023).

21. Geirinhas, J. L. et al. Recent increasing frequency of compound summer drought and heatwaves in Southeast Brazil. *Environ. Res. Lett.* **16**, 034036 (2021).

22. Wang, C. et al. Characteristic changes in compound drought and heatwave events under climate change. *Atmos. Res.* **305**, 107440 (2024).

23. Meng, Y., Hao, Z., Zhang, Y. & Feng, S. The 2022-like compound dry and hot extreme in the Northern Hemisphere: Extremeness, attribution, and projection. *Atmos. Res.* **295**, 107009 (2023).

24. Mukherjee, S., Mishra, A. K., Ashfaq, M. & Kao, S. C. Relative effect of anthropogenic warming and natural climate variability to changes in Compound drought and heatwaves. *J. Hydrol.* **605**, 127396 (2022).

25. Chancel, L. Global carbon inequality over 1990–2019. *Nat. Sustain.* **5**, 931–938 (2022).

26. Fischer, E. M. & Knutti, R. Anthropogenic contribution to global occurrence of heavy-precipitation and high-temperature extremes. *Nat. Clim. Chang.* **5**, 560–564 (2015).

27. Alizadeh, M. R. et al. Increasing heat-stress inequality in a warming climate. *Earth's Futur.* **10**, e2021EF002488 (2022).

28. Wei, T. et al. Developed and developing world responsibilities for historical climate change and CO2 mitigation. *Proc. Natl. Acad. Sci. USA.* **109**, 12911–12915 (2012).

29. Soergel, B. et al. Combining ambitious climate policies with efforts to eradicate poverty. *Nat. Commun.* **12**, 2342 (2021).

30. Sanders, B. F. et al. Large and inequitable flood risks in Los Angeles, California. *Nat. Sustain.* **6**, 47–57 (2023).

31. Castro, L. C. O. et al. Future climate risk from compound events. *Nat. Clim. Chang.* **8**, 80–91 (2018).

32. Smiley, K. T. et al. Social inequalities in climate change-attributed impacts of Hurricane Harvey. *Nat. Commun.* **13**, 3418 (2022).

33. Winsemius, H. C. et al. Disaster risk, climate change, and poverty: Assessing the global exposure of poor people to floods and droughts. *Environ. Dev. Econ.* **23**, 328–348 (2018).

34. Hersbach, H. et al. The ERA5 global reanalysis. *Q. J. R. Meteorol. Soc.* **146**, 1999–2049 (2020).

35. Zhang, Y., Mao, G., Chen, C., Shen, L. & Xiao, B. Population exposure to compound droughts and heatwaves in the observations and ERA5 reanalysis data in the Gan River Basin, China. *Land* **10**, 1021 (2021).

36. Beck, H. E. et al. MSWep v2 Global 3-hourly 0.1° precipitation: methodology and quantitative assessment. *Bull. Am. Meteorol. Soc.* **100**, 473–500 (2019).

37. Gelaro, R. et al. The modern-era retrospective analysis for research and applications, version 2 (MERRA-2). *J. Clim.* **30**, 5419–5454 (2017).

38. CPC. *Climate Prediction Center (CPC) Global Land Surface Air Temperature Analysis*. (2017).

39. Webb, R., Rosenzweig, C. E. & Levine, E. R. Global soil texture and derived water-holding capacities (Webb et al.). Data set. https://doi.org/10.3334/ORNLDAAC/548 (Oak Ridge National Laboratory Distributed Active Archive Center, Oak Ridge, TN, USA, 2000).

40. Zhang, B., Wang, S., Zscheischler, J. & Moradkhani, H. Higher exposure of poorer people to emerging weather whiplash in a warmer world. *Geophys. Res. Lett.* **50**, e2023GL105640 (2023).

41. Donat, M. G., Lowry, A. L., Alexander, L. V., O'Gorman, P. A. & Maher, N. More extreme precipitation in the world's dry and wet regions. *Nat. Clim. Chang.* **6**, 508–513 (2016).

42. Rentschler, J. & Leonova, N. Global air pollution exposure and poverty. *Nat. Commun.* **14**, 4432 (2023).

43. Wells, N., Goddard, S. & Hayes, M. J. A self-calibrating Palmer drought severity index. *J. Clim.* **17**, 2335–2351 (2004).

44. Thornthwaite, C. W. An approach toward a rational classification of climate. *Soil Sci* **66**, 77 (1948).

45. You, J. & Wang, S. Higher probability of occurrence of hotter and shorter heat waves followed by heavy rainfall. *Geophys. Res. Lett.* **48**, e2021GL094831 (2021).

46. Mukherjee, S., Mishra, A. K., Zscheischler, J. & Entekhabi, D. Interaction between dry and hot extremes at a global scale using a cascade modeling framework. *Nat. Commun.* **14**, 277 (2023).

47. Wang, J. et al. Anthropogenically-driven increases in the risks of summertime compound hot extremes. *Nat. Commun.* **11**, 528 (2020).

48. Yuan, X. et al. A global transition to flash droughts under climate change. *Science* **380**, 187–191 (2023).

Author contributions
B.Z. analyzed the data, interpreted the results, and drafted the manuscript; S.W. designed the study and edited the manuscript; L.S. reviewed and edited the manuscript.

Competing interests
The authors declare no competing interests.

Additional information
Supplementary information The online version contains supplementary material available at https://doi.org/10.1038/s43247-024-01894-7.

Correspondence and requests for materials should be addressed to Shuo Wang.

Peer review information *Communications Earth & Environment* thanks and the other, anonymous, reviewer(s) for their contribution to the peer review of this work. Primary Handling Editors: Charlotte Kendra Gotangco Gonzales, Martina Grecequet and Aliénor Lavergne. [A peer review file is available.]

Reprints and permissions information is available at http://www.nature.com/reprints

Publisher's note Springer Nature remains neutral with regard to jurisdictional claims in published maps and institutional affiliations.